Electrochimica Acta 218 (2016) 149–155

Contents lists available at ScienceDirect

Electrochimica Acta

journal homepage: www.elsevier.com/locate/electacta

# Rapid self-heating and internal temperature sensing of lithium-ion batteries at low temperatures

Guangsheng Zhang[a], Shanhai Ge[b], Terrence Xu[b], Xiao-Guang Yang[a], Hua Tian[a], Chao-Yang Wang[a,b,*]

[a] Department of Mechanical and Nuclear Engineering and Electrochemical Engine Center (ECEC), The Pennsylvania State University, University Park, PA 16802, USA
[b] EC Power, 341 Science Park Road, State College, PA 16803, USA

ARTICLE INFO

*Article history:*
Received 26 August 2016
Accepted 22 September 2016
Available online 23 September 2016

*Keywords:*
Self-heating lithium-ion battery
rapid self-heating
internal temperature sensing
low temperatures

ABSTRACT

The recently discovered self-heating lithium-ion battery structure provided a practical solution to the poor performance at subzero temperatures that has hampered battery technology for decades. Here we report an improved self-heating lithium-ion battery (SHLB) that heats from −20 °C to 0 °C in 12.5 seconds, or 56% more rapidly, while consuming 24% less energy than that reported previously. We reveal that a nickel foil heating element embedded inside a SHLB cell plays a dominant role in self-heating and we experimentally demonstrate that a 2-sheet design can achieve dramatically accelerated self-heating due to more uniform internal temperature distribution. We also report, for the first time, that this embedded nickel foil can simultaneously perform as an internal temperature sensor (ITS) due to the perfectly linear relationship between the foil's electrical resistance and temperature.



## 1. Introduction

Although high energy density and durability have made lithium-ion batteries the dominant power source for applications from consumer electronics to electric vehicles (EVs) [1,2], unsolved challenges remain [3,4]. Significant power loss at subzero temperatures due to sluggish charge-transfer kinetics, slow solid-state diffusion of lithium in electrode materials, reduced electrolyte diffusivity and conductivity, and high solid-electrolyte interface (SEI) resistance [5–9] have proved especially troublesome for the expanding EV industry. These limitations dramatically reduce driving range [10,11] and prohibit regeneration and fast charging [4,12–14] in winter, vulnerabilities that greatly exacerbate the driver's range anxiety [15].

For the last two decades, researchers have attempted to overcome the low-temperature power challenge by reformulating electrolyte for low temperature applications [3,16–19]. While this approach may mitigate electrolyte related issues, it cannot address solid-state diffusion of lithium in the electrode, a major limiting factor [5,9]. Electrolytes reformulated specifically for low temperature applications also unfortunately compromise performance at higher temperatures. Hybridization of lithium-ion battery with high power devices such as supercapacitors has recently been explored [20]. This approach ensures high power output at system level in a wide range of temperatures, but system design and control are more complicated than that with only one type of power sources, and overall energy density is reduced. Preheating of the battery is another feasible approach used in virtually all commercial electric vehicles. Various internal heating strategies have been evaluated [21], including internal core heating through alternating currents (AC) [22–25], internal resistive heating, convective heating and mutual pulse heating [26], as well as external heating strategies such as using air, liquid or phase change materials [21,26]. Although these heating methods are prevalent, they are time- and energy-consuming, i.e. taking tens of minutes and consuming ~10% battery energy. Some also require complicated heating circuits [22,23,26].

Our group recently discovered a self-heating lithium-ion battery (SHLB) structure [27,28] that is simple to manufacture yet effective, wherein nickel foil embedded inside the Li-ion cell enables rapid, efficient self-heating. As reported in [27], the process requires only 20 seconds to warm up a SHLB cell from −20 °C to 0 °C while consuming 3.8% of capacity. In addition, cycle tests demonstrate that SHLB cells have excellent durability and reliability, surviving 500 self-heating test cycles at −30 °C, 1,000 cycles at 45 °C and 2,500 cycles at 25 °C.

* Corresponding author.
*E-mail address:* cxw31@psu.edu (C.-Y. Wang).

http://dx.doi.org/10.1016/j.electacta.2016.09.117
0013-4686/

Here we report, for the first time, a major improvement over the previously published SHLB structure, incorporating a two-sheet Ni foil design that enables more rapid and efficient self-heating, and we introduce novel use of this nickel foil for internal temperature sensing (ITS). This significant improvement now provides cell heating in only 12.5 seconds from −20 °C to 0 °C and consumes only 2.9% capacity. Finally, we perform thermal analysis and ITS measurements to lend fundamental insight into the rapid self-heating process.

## 2. Experimental

### 2.1. Working principle of rapid self-heating and internal temperature sensing

Fig. 1a shows a schematic of the new SHLB structure and Fig. 1b shows its electric circuit representation. Nickel foil, as shown in Fig. 1a and detailed in [27], is embedded inside a lithium-ion cell. One end of the nickel foil is welded to negative (anode) terminal of the cell and the other end extends outside the cell as a third terminal, called the activation (ACT) terminal. A temperature-controlled switch is placed between the ACT terminal and positive (cathode) terminal. At a low temperature the switch is turned on and electrical current flows through the nickel foil, generating substantial internal heat to warm up the cell (heating mode). Since the nickel foil is embedded inside the cell and no electrical energy is consumed on the external circuit, all energy consumed during this self-heating process is very efficiently used to warm up the cell. When the cell temperature rises to a set value, the switch turns off automatically, reverting the cell to the baseline mode where an external load is connected between the positive and negative terminals and no current flows through the nickel foil. While the previous configuration placed the switch between negative terminal and ACT terminal [27], this new design simplifies the self-heating process, offering 100% conversion of electrical energy into heat within the cell.

In addition to the altering switch connection, we embed a second nickel foil sheet in this new design. Fig. 1c shows schematic location of nickel foils in the thickness direction for SHLB cells with 1-sheet design (previous work) and new 2-sheet design (this work). Dashed arrows in the schematics indicate flow of heat from nickel foil to adjacent battery materials. Internal heat generation with 2-sheet design is expected to be more uniform than the 1-sheet design, making the self-heating process more rapid and more efficient. Note that the two designs closely resemble each other in external appearance since nickel foil sheets are welded together in parallel within the 2-sheet cell.

The electrical resistance of nickel foil is designed according to SHLB capacity and size. Fig. 1d shows resistance of nickel foil in a SHLB cell at different temperatures. Note that there exists a linear relation between foil resistance and temperature. Based on this linear correlation, foil temperature can be simply obtained by measuring its resistance. Therefore, the same nickel foil used in SHLB as heating element can be simultaneously used as an internal temperature sensor. This new capability provides a convenient yet powerful diagnostic tool to investigate the self-heating process as well as other battery operations involving significant internal temperature rise.

### 2.2. Fabrication of SHLB cells

Self-heating pouch cells were fabricated using $LiNi_{0.6}Co_{0.2}Mn_{0.2}O_2$ as cathode active material and graphite (Nippon Carbon) as anode active material, with 1 M of $LiPF_6$ dissolved in ethylene carbonate/ethyl methyl carbonate (3:7 by weight) and 2% vinylene carbonate as electrolyte. Separator was Celgard-2325 microporous trilayer membrane with thickness of 25 μm. The

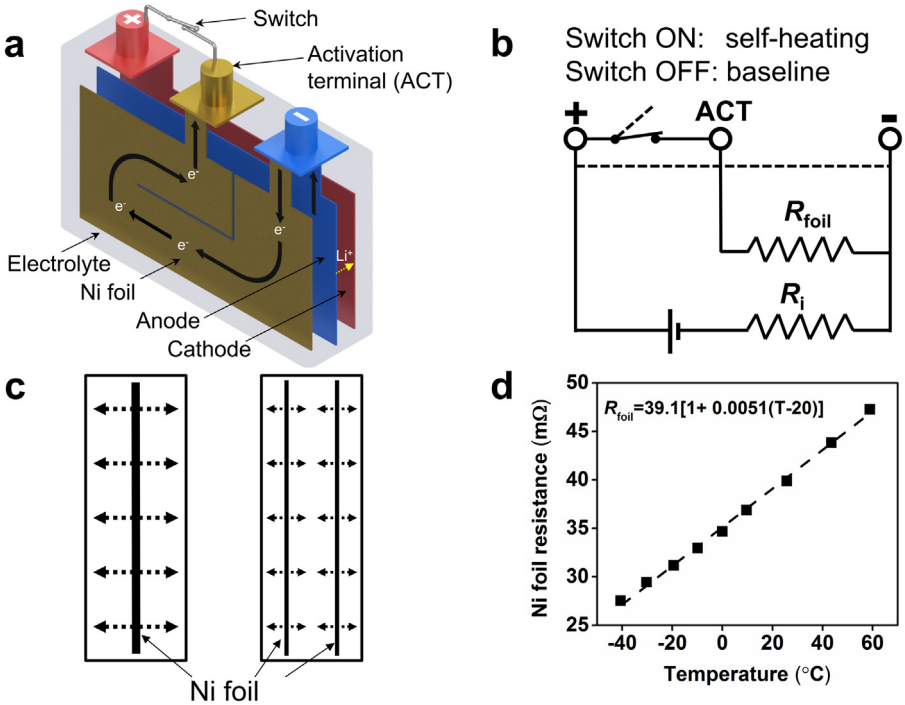


**Fig. 1.** Working principle of rapid self-heating Li-ion battery. (a) Schematic of cell structure with embedded Ni foil and a switch between positive terminal and activation terminal. (b) Electric circuit representation of self-heating process. (c) Schematic of Ni foil location in self-heating cells with 1-sheet design (Ni foil in the middle of cell thickness, arrows indicate heat flow from Ni foil to electrode layers (not drawn here)) and 2-sheet design (2 pieces of Ni foil at 1/4 and 3/4 of cell thickness). (d) Linear relation between Ni foil resistance and temperature (to enable internal temperature sensing based on electrical resistance measurement).

capacity ratio of negative to positive electrode was designed at 1.2. The cathodes were prepared by coating NMP based slurry onto 15 μm thick Al foil, whose dry material consisted of $LiNi_{0.6}Co_{0.2}Mn_{0.2}O_2$ (91.5 wt.%), Super-C65 (Timcal) (4.4 wt.%) and PVdF (Hitachi) (4.1 wt.%) as a binder. The anodes were prepared by coating deionized (DI) water-based slurry onto 10 μm thick Cu foil, whose dry material consisted of graphite (95.4 wt.%), Super-C65 (1.0 wt.%), SBR (JSR) (2.2 wt.%) and CMC (Nippon Paper) (1.4 wt.%). The total thickness of each cathode and anode layer is 105 um and 114 um, respectively (double-sided and including the current-collecting foil thickness).

The cells contain a stack of 34 anode and 33 cathode layers. Nickel foil with resistance of 39 milli-Ohm at 20 °C is coated with a thin (28 μm) backing material of polyethylene terephthalate for electrical insulation and sandwiched between 2 single-sided anode layers. This 3-layer assembly is then stacked in the middle of the electrode stack for 1-sheet cell. One tab of the metal foil is electrically connected to the negative terminal, being welded together with the tabs of all anode layers. The other tab extends outside the cell to form a third terminal, the activation (ACT) terminal. Similar 3-layer assemblies are used in the 2-sheet cell, but each nickel foil has resistance of 78 milli-Ohm at 20 °C and two pieces of 3-layer assemblies are stacked at $^1/_4$ and $^3/_4$ of cell thickness. By connecting the two pieces of assemblies in parallel, the total resistance of heating element in 2-sheet cell is the same as the 1-sheet cell.

Each cell has a 152 × 75 mm footprint area and has 10 Ah nominal capacity (relative to which all C-rates in this report are given). The 1-sheet cell weighs 208 g and the 2-sheet cell weighs 210 g. They have specific energy of 170 Wh/kg when discharged at C/3 at room temperature. The total Ni foils we add in an ACB cell have the same weight and volume between 1-sheet and 2-sheet designs as each foil thickness in the 2-sheet design is exactly half of that in the 1-sheet design, weighing ~100 g per kWh battery with a cost of $1/kWh based upon Nickel price of $10/kg. Compared to the best specific energy of current Li-ion battery systems, i.e. 150 Wh/kg battery-system, and an assumed battery cost of $250/kWh, the added weight and cost due to Ni foils are 1.5% and 0.4% of the baseline battery [27].

### 2.3. Self-heating test protocol

For self-heating tests in this study, cells were firstly fully charged at room temperature by a battery tester (BT2000, Arbin), and then cooled at desired ambient temperature by an environmental chamber (Tenney T10c, Thermal Product Solutions) for at least 6 hours to reach thermal equilibrium. A T type thermocouple (SA1-T, OMEGA Engineering) was placed at the center of cell outer surface. To obtain experimental data for detailed investigation, including self-heating current and cell voltage, the battery tester was used as an on-off switch by setting voltage between positive terminal and ACT terminal at 0 V during the self-heating process until cell surface temperature reached −5 °C, the same practice used in our previous work [27]. The voltage between positive terminal and negative terminal was also monitored by the battery tester and designated as cell voltage in the present work. The nickel foil resistance can be determined by the voltage drop measured between the ACT terminal and negative terminal divided by current flowing in the self-heating mode.

## 3. Results and Discussion

Fig. 2a, 2b, and 2c show results of voltage, current and surface temperature of the 2-sheet SHLB cell during self-heating from −20 °C, respectively. The results for 1-sheet self-heating cell are shown in Fig. 2d-2f for comparison. Open circuit voltage of cell ($V_{oc}$) is estimated as a linear line during the self-heating process and plotted together with cell voltage to help understand overpotential during self-heating. It can be seen that cell voltage ($V_{cell}$) drops immediately when self-heating begins, while the self-heating current jumps to ~8C (1C equals to 10A). The high current flowing though nickel foil and electrodes generates considerable heat, causing rapid increase of cell temperature. The temperature increase in turn leads to decreased cell internal resistance, reducing overpotential of electrochemical reactions and causing recovery of cell voltage. While voltage and current of the two cells show similar trends, surface temperature of the 2-sheet cell increases much faster than the 1-sheet cell, with complete self-heating in only 12.5 seconds for the 2-sheet cell. This is 56% more

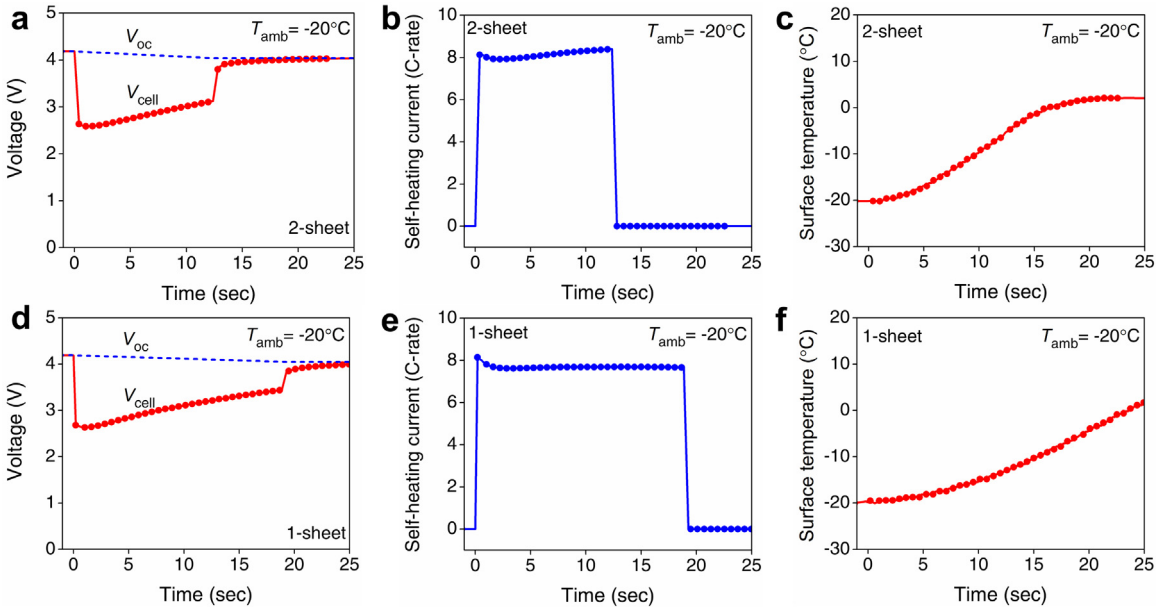


**Fig. 2.** Voltage, current and surface temperature of 1-sheet and 2-sheet cells during self-heating from −20 °C. (a)(d) Measured cell voltage ($V_{cell}$) and estimated open circuit voltage ($V_{OC}$). (b)(e) Self-heating current in C-rate (1C = 10A). (c)(f) Outer surface temperature.

rapid than the previously reported result [27]. Note that the cell surface temperature is −5 °C at the end of self-heating, but continues to increase to above 0 °C due to lagging response in the surface temperature. Similar trends are also observed in self-heating from −30 °C and −40 °C, as shown in Fig. 3 and Fig. 4 respectively. These results clearly demonstrate the superb advantage of the 2-sheet design.

During the self-heating process, heat is generated both from ohmic heating on the nickel foil and from electrochemical reactions, and they can be quantitatively de-convoluted. As labelled in Fig. 5a, the heating power from electrochemical operation can be estimated by $(V_{oc} - V_{cell})^*I$ and ohmic heating from nickel foil by $V_{cell}{}^*I$, where $I$ is the self-heating current. Temporal variations of the heating power from electrochemical reaction and from nickel foil are plotted in Fig. 5a and Fig. 5c for 2-sheet cell and 1-sheet cell, respectively. The relative heating power in percentage is further plotted in Fig. 5b and Fig. 5d. It can be seen that heat from the nickel foil plays a dominant role even from the beginning of self-heating, accounting for more than 60% of total heat generation, and becoming even more dominant as self-heating proceeds, accounting for 77% of total heat for the 2-sheet cell and 85% for the 1-sheet cell by the end of self-heating. In comparison, percentage of heat from electrochemical reaction decreases from 40% to 23% and 15%, respectively. Similar characteristics are also seen in self-heating from −30 °C and −40 °C, as shown in Fig. 6 and Fig. 7, respectively. The increasing dominance of ohmic heat from nickel foil during self-heating can be attributed to the opposite effects of temperature on foil

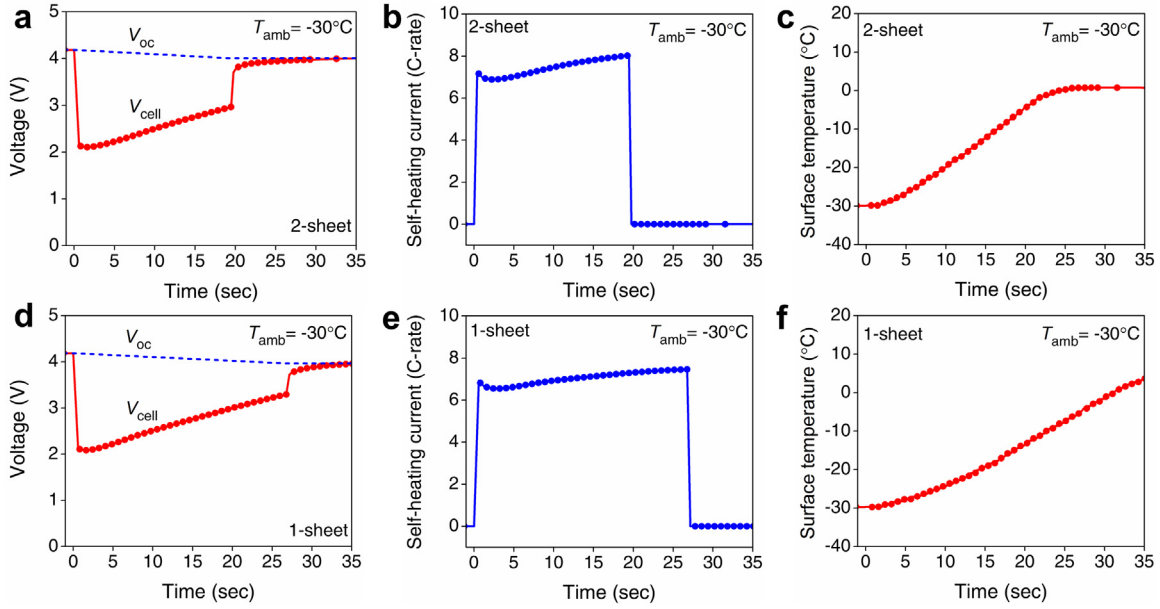


**Fig. 3.** Voltage, current and surface temperature of 1-sheet and 2-sheet cells during self-heating from −30 °C. (a)(d) Measured cell voltage ($V_{cell}$) and estimated open circuit voltage ($V_{OC}$). (b)(e) Self-heating current in C-rate (1C = 10A). (c)(f) Surface temperature.

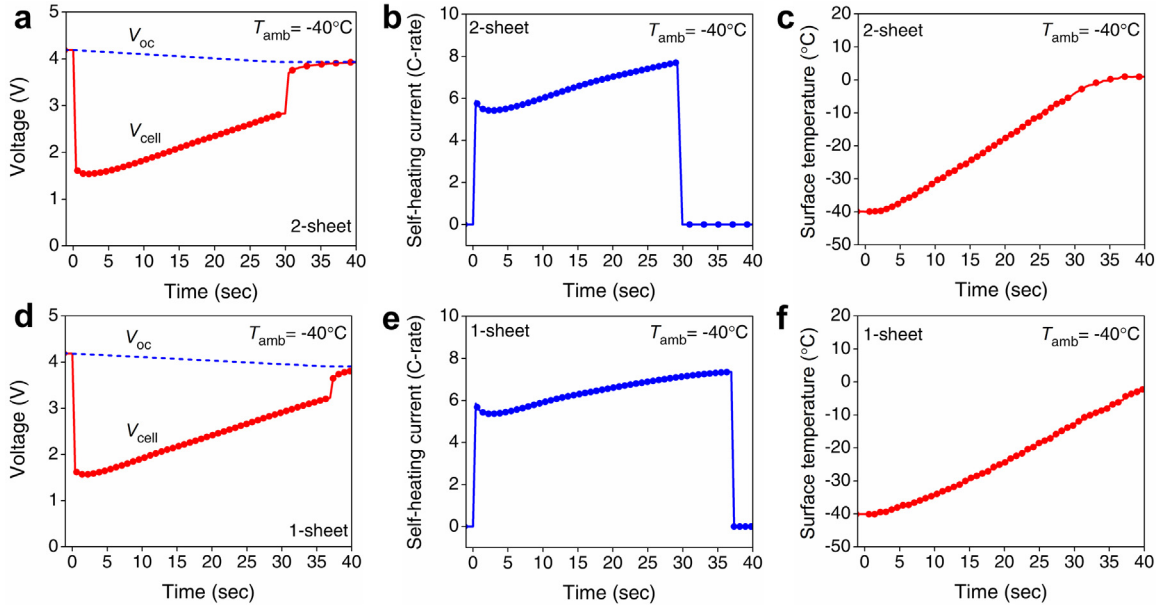


**Fig. 4.** Voltage, current and surface temperature of 1-sheet and 2-sheet cells during self-heating from −40 °C. (a)(d) Measured cell voltage and estimated open circuit voltage. (b)(e) Self-heating current in C-rate (1C = 10A). (c)(f) Surface temperature.

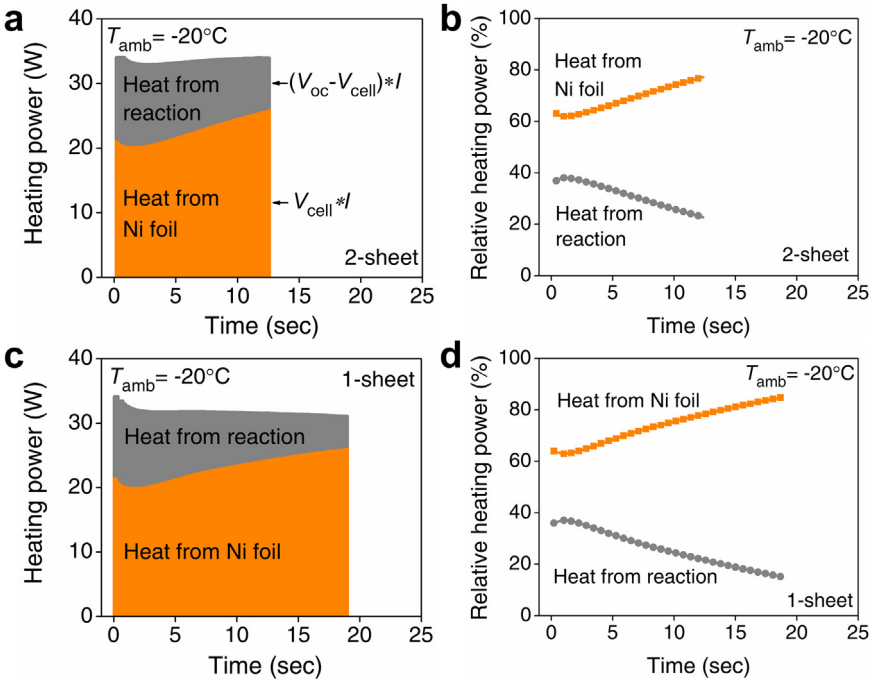


**Fig. 5.** Breakdown of heating power from electrochemical reactions and from nickel foil during self-heating from −20 °C. (a)(c) Heating power (absolute). (b)(d) Relative heating power.

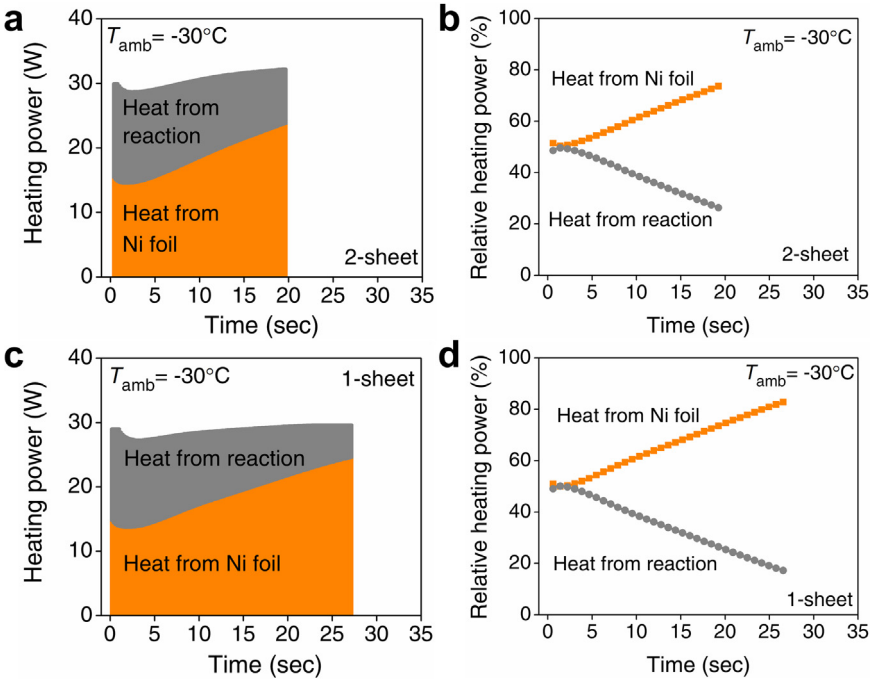


**Fig. 6.** Breakdown of heating power from electrochemical reactions and from nickel foil during self-heating from −30 °C. (a)(c) Heating power. (b)(d) Relative heating power.

resistance and cell internal resistance. Heating power from nickel foil and that from electrochemical reaction can be also interpreted by $I^2*R_{foil}$ and $I^2*R_i$, respectively, in which $R_{foil}$ and $R_i$ are nickel foil resistance and cell internal resistance. On one hand, the nickel foil resistance increases with temperature, generating more ohmic heat. On the other hand, the cell internal resistance drops significantly with temperature due to enhanced reaction kinetics and transport properties [9,29,30], thus reducing heating power. The quantitative heat generation data suggest that the embedded nickel foil plays a key role in the rapid self-heating process and is the main reason the SHLB cell requires only a tiny fraction of the heating time of existing methods [26].

The results of self-heating from −30 °C and −40 °C are similar to that from −20 °C, except that longer self-heating time and more energy consumption are needed due to lower initial temperatures. Fig. 8a summarizes self-heating time for each cell. The 2-sheet cell self-heats from −30 °C and −40 °C in 19.2 and 29.4 seconds, results that are 54% and 45% faster than previously reported, and also

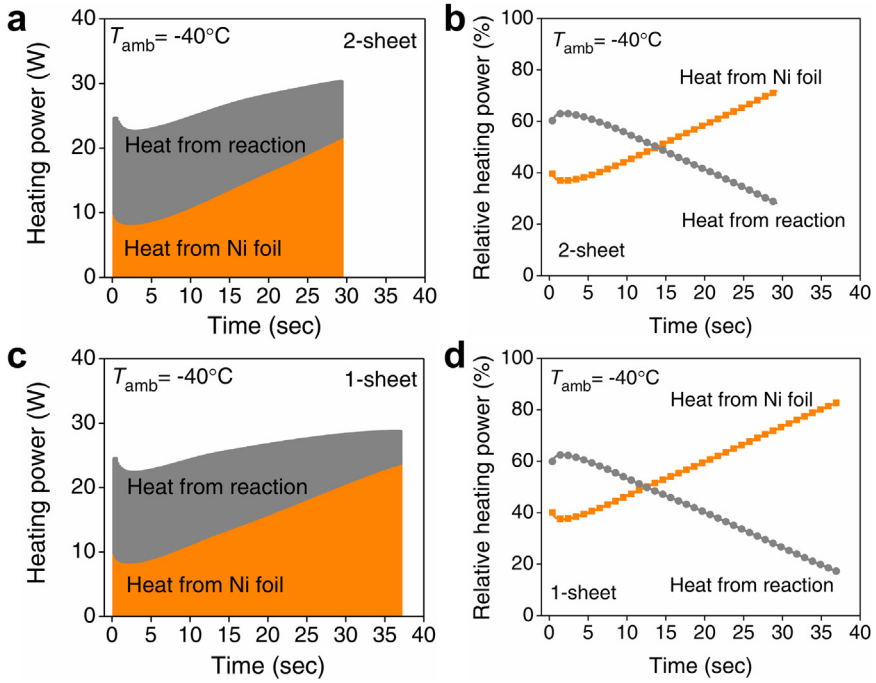


**Fig. 7.** Breakdown of heating power from electrochemical reactions and from nickel foil during self-heating from −40 °C. (a)(c) Heating power. (b)(d) Relative heating power.

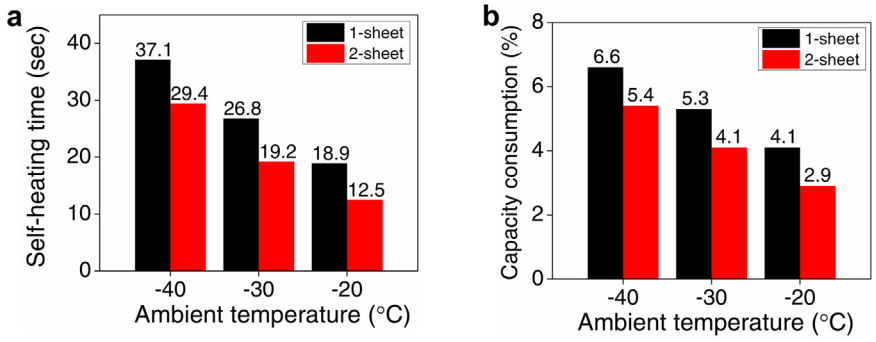


**Fig. 8.** Self-heating time and capacity consumption of 1-sheet and 2-sheet cells at different ambient temperatures. (a) Self-heating time. (b) Capacity consumption.

consistently more rapid than 1-sheet cell with similar design in this study, namely 40% and 26% from −30 °C and −40 °C, respectively. Accordingly, the capacity consumption during self-heating is consistently less for 2-sheet cell, 18%-24% compared with previous results, as shown in Fig. 8b. These results clearly demonstrate the advantage of 2-sheet design in rapid self-heating.

The more rapid self-heating of SHLB cell with 2-sheet design is expected due to distributed heat generation and more uniform temperature distribution inside the cell. This hypothesis can be experimentally confirmed by treating the nickel foil as an internal temperature sensor. Fig. 9 shows the foil temperature and cell outer surface temperature during self-heating from −20 °C, −30 °C and −40 °C. The difference between foil and surface temperatures represents the maximum temperature gradient existing inside the cell. It can be seen that foil temperature increases much faster than the surface temperature in all cases, for both cell designs. However,

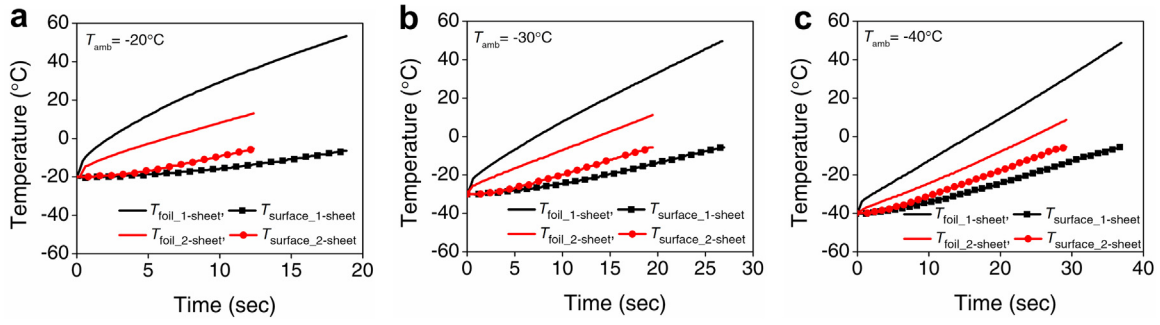


**Fig. 9.** Surface and foil temperatures of 1-sheet and 2-sheet cells during self-heating from (a) −20 °C. (b) −30 °C. (c) −40 °C.

the temperature difference in the 2-sheet cell is nearly three to four times smaller than that in the 1-sheet cell. This smaller temperature gradient in the 2-sheet cell significantly reduces the time required for cell surface warmup, accelerating self-heating. Note also that the temperature gradient during self-heating is smaller from lower ambient temperatures, probably because longer heating time permits more thermal spreading.

## 4. Conclusions

We have experimentally demonstrated accelerated self-heating of a lithium-ion battery from low temperatures, a major improvement of the recently discovered SHLB structure, to overcome the long-standing low temperature challenge. Implementation of a 2-sheet design instead of the previously published 1-sheet design increased self-heating speed by 45%-56% and reduced energy consumption by 18%-24% in the ambient temperature range of −40 °C to −20 °C. Through quantitative breakdown of heat generation, we have elucidated that the nickel foil embedded inside a SHLB cell played a key role in the rapid self-heating process. The new design generates considerably more heat than electrochemical reactions, even more so as self-heating proceeds, due to the opposite trends of nickel foil resistance and cell internal resistance with increasing temperature. We have also demonstrated, for the first time, new potential offered by internal temperature sensing using the same embedded nickel foil owing to the excellent linear relation between its resistance and temperature. With this new experimental capability, we confirmed that the 2-sheet design yields more rapid self-heating than the 1-sheet design due to much more uniform temperature distribution. The simultaneous capabilities of rapid self-heating and internal temperature sensing, as demonstrated through 2-sheet SHLB cells in this work, could open up a class of smart batteries where performance, health and safety can be actively regulated rather than passively endured for challenging applications such as all-climate electric vehicles. Further efforts, such as optimizing cell design through electrochemical-thermal coupled models [31], developing more efficient self-heating protocols, experimenting with different metal foil materials such as aluminium, and applying this technique to other battery chemistries, are warranted.

## Acknowledgment

Financial support of this work by EC Power is gratefully acknowledged.

## References

[1] M. Armand, J.M. Tarascon, Building better batteries, Nature 451 (2008) 652–657.
[2] D.H.C. Wong, J.L. Thelen, Y. Fu, D. Devaux, A.A. Pandya, V.S. Battaglia, N.P. Balsara, J.M. DeSimone, Nonflammable perfluoropolyether-based electrolytes for lithium batteries, Proceedings of the National Academy of Sciences 111 (2014) 3327–3331.
[3] S.R. Ein-Eli, R. Thomas, T.J. Chadha, Li-ion battery electrolyte formulated for low-temperature applications, Journal of The Electrochemical Society 144 (1997) 823–829.
[4] T. Waldmann, B.-I. Hogg, M. Kasper, S. Grolleau, C.G. Couceiro, K. Trad, B.P. Matadi, M. Wohlfahrt-Mehrens, Interplay of operational parameters on lithium deposition in lithium-ion cells: systematic measurements with reconstructed 3-electrode pouch full cells, Journal of The Electrochemical Society 163 (2016) A1232–A1238.
[5] C.K. Huang, J.S. Sakamoto, J. Wolfenstine, S. Surampudi, The limits of low-temperature performance of Li-ion cells, Journal of The Electrochemical Society 147 (2000) 2893–2896.
[6] H.-p. Lin, D. Chua, M. Salomon, H.-C. Shiao, M. Hendrickson, E. Plichta, S. Slane, Low-temperature behavior of Li-ion cells, Electrochemical and Solid-State Letters 4 (2001) A71–A73.
[7] L.O. Valoen, J.N. Reimers, Transport properties of LiPF6-based Li-ion battery electrolytes, Journal of the Electrochemical Society 152 (2005) A882–A891.
[8] K.L. Gering, Low-temperature performance limitations of lithium-ion batteries, ECS Transactions 1 (2006) 119–149.
[9] Y. Ji, Y. Zhang, C.Y. Wang, Li-ion cell operation at low temperatures, Journal of the Electrochemical Society 160 (2013) A636–A649.
[10] K. Stutenberg, Advanced Technology Vehicle Lab Benchmarking—Level 1, 2014 U.S. DOE Vehicle Technologies Program Annual Merit Review and Peer Evaluation Meeting, June 16–20, 2014, Washington, DC, 2014.
[11] AAA, Extreme temperatures affect electric vehicle driving range, AAA says. http://newsroom.aaa.com/2014/03/extreme-temperatures-affect-electric-vehicle-driving-range-aaa-says/, 2014 (accssed 04/20/2016).
[12] M. Ouyang, Z. Chu, L. Lu, J. Li, X. Han, X. Feng, G. Liu, Low temperature aging mechanism identification and lithium deposition in a large format lithium iron phosphate battery for different charge profiles, Journal of Power Sources 286 (2015) 309–320.
[13] M. Petzl, M. Kasper, M.A. Danzer, Lithium plating in a commercial lithium-ion battery—A low-temperature aging study, Journal of Power Sources 275 (2015) 799–807.
[14] S.S. Zhang, K. Xu, T.R. Jow, The low temperature performance of Li-ion batteries, Journal of Power Sources 115 (2003) 137–140.
[15] J. Neubauer, E. Wood, The impact of range anxiety and home, workplace, and public charging infrastructure on simulated battery electric vehicle lifetime utility, Journal of Power Sources 257 (2014) 12–20.
[16] S.S. Zhang, K. Xu, T.R. Jow, A new approach toward improved low temperature performance of Li-ion battery, Electrochemistry Communications 4 (2002) 928–932.
[17] M.C. Smart, B.V. Ratnakumar, L.D. Whitcanack, K.B. Chin, S. Surampudi, H. Croft, D. Tice, R. Staniewicz, Improved low-temperature performance of lithium-ion cells with quaternary carbonate-based electrolytes, Journal of Power Sources 119–121 (2003) 349–358.
[18] B.K. Mandal, A.K. Padhi, Z. Shi, S. Chakraborty, R. Filler, New low temperature electrolytes with thermal runaway inhibition for lithium-ion rechargeable batteries, Journal of Power Sources 162 (2006) 690–695.
[19] S. Li, X. Li, J. Liu, Z. Shang, X. Cui, A low-temperature electrolyte for lithium-ion batteries, Solid State Ionics 21 (2015) 901–907.
[20] P. Keil, M. Englberger, A. Jossen, Hybrid energy storage systems for electric vehicles: An experimental analysis of performance improvements at subzero temperatures, IEEE Trans. Veh. Technol. 65 (2016) 998–1006.
[21] J. Jaguemont, L. Boulon, Y. Dubé, A comprehensive review of lithium-ion batteries used in hybrid and electric vehicles at cold temperatures, Applied Energy 164 (2016) 99–114.
[22] A. Vlahinos, A.A. Pesaran, Energy efficient battery heating in cold climates, SAE Technical Paper 2002-01-1975 (2002) 1–8.
[23] T.A. Stuart, A. Hande, HEV battery heating using AC currents, Journal of Power Sources 129 (2004) 368–378.
[24] J. Zhang, H. Ge, Z. Li, Z. Ding, Internal heating of lithium-ion batteries using alternating current based on the heat generation model in frequency domain, Journal of Power Sources 273 (2015) 1030–1037.
[25] M. Zuniga, J. Jaguemont, L. Boulon, Y. Dube, Heating lithium-ion batteries with bidirectional current pulses, IEEE Vehicle Power and Propulsion Conference (VPPC) (2015) 1–6.
[26] Y. Ji, C.Y. Wang, Heating strategies for Li-ion batteries operated from subzero temperatures, Electrochimica Acta 107 (2013) 664–674.
[27] C.Y. Wang, G. Zhang, S. Ge, T. Xu, Y. Ji, X.G. Yang, Y. Leng, Lithium-ion battery structure that self-heats at low temperatures, Nature 529 (2016) 515–518.
[28] C.Y. Wang, T. Xu, S. Ge, G. Zhang, X.G. Yang, Y. Ji, A fast rechargeable lithium-ion battery at subfreezing temperatures, Journal of The Electrochemical Society 163 (2016) A1944–A1950.
[29] S.S. Zhang, K. Xu, T.R. Jow, Electrochemical impedance study on the low temperature of Li-ion batteries, Electrochimica Acta 49 (2004) 1057–1061.
[30] A. Senyshyn, M.J. Mühlbauer, O. Dolotko, H. Ehrenberg, Low-temperature performance of Li-ion batteries: The behavior of lithiated graphite, Journal of Power Sources 282 (2015) 235–240.
[31] X.G. Yang, G. Zhang, C.Y. Wang, Computational design and refinement of self-heating lithium ion batteries, Journal of Power Sources 328 (2016) 203–211.